High expression of G3BP1 is associated with poor prognosis in breast invasive carcinoma

JINGJING LI[1*], ZHIQIANG ZONG[1*], JIAN SHEN[1*], JIAHAO WANG[2*], XUAN ZHOU[1], WEI SHI[1], JIA LI[2], HONG ZHAO[3], YUNWEN YAN[4] and FANFAN LI[1]

[1]Department of Oncology, The Second Affiliated Hospital of Anhui Medical University, Hefei, Anhui 230601, P.R. China; [2]Department of General Surgery, The Second Affiliated Hospital of Anhui Medical University, Hefei, Anhui 230601, P.R. China; [3]Department of Radiology, The Second Affiliated Hospital of Anhui Medical University, Hefei, Anhui 230601, P.R. China; [4]Department of Breast Surgery, The First Affiliated Hospital of Anhui Medical University, Hefei, Anhui 230022, P.R. China

Received May 14, 2025; Accepted September 16, 2025

DOI: 10.3892/ol.2025.15434

Abstract. Breast invasive carcinoma (BRCA) is the most common type of cancer affecting women worldwide. Biomarkers such as estrogen receptor, progesterone receptor and HER2 are currently utilized in clinical practice for breast cancer diagnosis; yet their sensitivity and specificity remain limited. However, Ras-GTPase-activating protein SH3 domain-binding protein 1 (G3BP1), an RNA-binding protein, has been implicated in tumor progression in various cancers, yet its clinical relevance and mechanistic role in BRCA still remain unclear. The present study integrated multi-omics data analysis and experimental validation to address this. G3BP1 mRNA and protein expression levels in BRCA were analyzed using The Cancer Genome Atlas, Tumor Immune Estimation Resource (TIMER) and Clinical Proteomic Tumor Analysis Consortium databases. Kaplan-Meier survival analysis and Cox regression were employed to evaluate the prognostic value of G3BP1. Gene set enrichment analysis (GSEA) was performed to identify associated signaling pathways and immune cell infiltration correlations were assessed using CIBERSORT and TIMER. Additionally, 38 samples of BRCA and adjacent normal tissue were collected for immunohistochemical (IHC) validation and diagnostic efficacy was evaluated using receiver operating characteristic (ROC) curves. G3BP1 was significantly upregulated in BRCA tissues at both mRNA and protein levels (P<0.05). High G3BP1 expression was associated with the advanced cancer lymph node stage (P=0.005) and a poor prognosis [overall survival, disease-free survival (DFS), distant metastasis-free survival and post-progression survival; all P<0.05]. Differential gene analysis identified 67 upregulated and 9 downregulated genes. GSEA revealed G3BP1 enrichment in key pathways such as PI3K/AKT/mTOR signaling and ubiquitin-mediated proteolysis. Immune analysis showed a significant positive association between G3BP1 and M2 macrophage infiltration (P<0.05) and a significant negative association between G3BP1 and $CD8^+$ T cells (P<0.05). IHC confirmed higher G3BP1 expression in BRCA compared with normal tissues (P<0.001), with an area under the ROC curve (AUC) of 0.777 and a 5-year DFS prediction AUC of 0.730. The present findings indicate that G3BP1 is a potential independent prognostic biomarker for BRCA. Its upregulation promotes tumor progression by activating the PI3K/AKT/mTOR signaling pathway and modulating the tumor immune microenvironment. These findings provide a theoretical foundation for targeting G3BP1 in BRCA diagnosis and immunotherapy.

Correspondence to: Dr Yunwen Yan, Department of Breast Surgery, The First Affiliated Hospital of Anhui Medical University, 218 Jixi Road, Hefei, Anhui 230022, P.R. China
E-mail: sweetmile@163.com

Professor Fanfan Li, Department of Oncology, The Second Affiliated Hospital of Anhui Medical University, 678 Furong Road, Hefei, Anhui 230601, P.R. China
E-mail: fflahykdx@163.com

*Contributed equally

Key words: Ras-GTPase-activating protein SH3 domain-binding protein 1, breast invasive carcinoma, prognosis, immunohistochemistry, bioinformatics

Introduction

Breast cancer is the most prevalent malignancy among women worldwide, with 2.26 million new cases reported in 2020 (accounting for 24.5% of all new cancer cases) and ~685,000 mortalities annually (1,2). Breast invasive carcinoma (BRCA) is the most prevalent malignant type of breast cancer, characterized by tumor cells penetrating the basement membrane of mammary ducts or lobules and infiltrating surrounding tissues, with the potential to metastasize to distant organs through the lymphatic system or hematogenous circulation (3). Although the widespread adoption of screening techniques and advances in comprehensive treatment have improved the 5-year survival rate of early-stage breast cancer to 90%, the 5-year survival rate for patients with metastatic breast

cancer remains <30% (4,5). Notably, treatment modalities such as intraoperative radiotherapy have shown a higher local recurrence risk compared with whole-breast radiotherapy in patients with early-stage breast cancer (6).

Current biomarkers, including estrogen receptor (ER), progesterone receptor (PR), HER2, programmed death-ligand 1 (PD-L1) and tumor mutation burden, exhibit limitations in their sensitivity and specificity (7). However, emerging multi-gene signatures, including the nine-long non-coding RNA prognostic model, require further validation for clinical use (8). The tumor immune microenvironment (TIME) influences BRCA progression, as M2 macrophages drive immunosuppression via C-X-C motif chemokine ligand 1-mediated PI3K/AKT/NF-κB activation, elevating PD-L1 expression levels (9). Additionally, in Traditional Chinese Medicine, it is believed that decoction therapies suppress metastasis by modulating the epithelial-to-mesenchymal transition (EMT) and immune cells such as CD4+ T, T-helper 1 and monocytic myeloid-derived suppressor cells (10).

Ras-GTPase-activating protein SH3 domain-binding protein 1 (G3BP1) is an RNA-binding protein (RBP) that serves a key role in regulating mRNA stability, stress granule (SG) formation and signal transduction (7). Emerging evidence has demonstrated that G3BP1 is frequently upregulated in various malignancies and contributes to tumor progression through multiple mechanisms: i) Serving as a core scaffold protein of SGs to promote tumor cell survival under chemotherapeutic or hypoxic stress conditions; ii) activating oncogenic signaling pathways such as PI3K/AKT/mTOR to enhance tumor cell proliferation and metastasis; and iii) modulating the infiltration and function of immune cells within the tumor microenvironment to establish an immunosuppressive niche (7,11,12).

Therefore, the present study aimed to investigate the association between G3BP1 expression and the clinicopathological characteristics and prognosis of BRCA, as well as elucidate the biological role of G3BP1 in BRCA. Utilizing multiple online databases, the differential expression of G3BP1 between BRCA tumor and normal tissues was compared, and the association between G3BP1 expression levels and clinicopathological features was assessed. Immunohistochemical (IHC) analysis was then performed at the tissue level to validate the expression patterns of G3BP1, while clinical follow-up data were analyzed to verify its prognostic value. Gene set enrichment analysis was performed to identify biological pathways associated with G3BP1, while immune infiltration analysis was performed to uncover the biological impact and potential mechanisms of G3BP1 in BRCA.

Materials and methods

Analysis of G3BP1 expression profiles across human tissues. To comprehensively characterize the expression profile of G3BP1 across transcriptional and proteomic hierarchies in human tissues, multi-omics data from publicly accessible repositories was leveraged. Pan-cancer mRNA expression of G3BP1 was interrogated using the Tumor Immune Estimation Resource (TIMER) database (https://cistrome.shinyapps.io/timer/) (13). Transcriptomic data from The Cancer Genome Atlas (TCGA; https://portal.gdc.cancer.gov/) BRCA project were analyzed to evaluate differential G3BP1 expression between breast tumor tissue and normal tissue. Proteomic quantification of G3BP1 in BRCA was performed using the Confirmatory Breast Cancer (CBC) cohort from Clinical Proteomic Tumor Analysis Consortium (CPTAC) dataset (https://cptac-data-portal.georgeton.edu/), with Z-scores representing standardized deviations relative to the median expression. IHC validation was conducted through the Human Protein Atlas (HPA) platform, for comparison of G3BP1 protein localization and intensity between malignant and non-malignant breast tissue. The specific image data for G3BP1 in breast cancer tissue can be accessed at: https://www.proteinatlas.org/ENSG00000145907-G3BP1/cancer/breast+cancer, and for normal breast tissue at: https://www.proteinatlas.org/ENSG00000145907-G3BP1/tissue/breast. All data and images regarding G3BP1 from the HPA are based upon work from the HPA consortium and are available under a CC BY-SA 4.0 license (14).

Differential expression analysis of G3BP1 and association between G3BP1 and clinicopathological variables. Differential expression of G3BP1 between tumor and adjacent normal tissues in TCGA-Breast Invasive Carcinoma collection (TCGA-BRCA) was evaluated using non-parametric statistical analyses. A Mann-Whitney U test was used for unpaired samples (tumor compared with normal tissue), while the Wilcoxon signed-rank test was used for paired samples. Associations between G3BP1 expression levels and clinicopathological variables, including age, sex, tumor (T) stage, lymph node (N) stage, metastasis (M) stage and pathological stage, were assessed using the Kruskal-Wallis test (for multi-group comparisons), followed by Dunn's post-hoc test with Benjamini-Hochberg correction for pairwise comparisons when a significant overall difference was observed ($P<0.05$), and Mann-Whitney U test (for two-group comparisons). $P<0.05$ was considered to indicate a statistically significant difference (Benjamini-Hochberg correction).

Survival analysis based on the expression of G3BP1 in BRCA. Kaplan-Meier survival analysis was performed to assess the prognostic value of G3BP1 expression in TCGA-BRCA collection, integrating RNA-sequencing data and clinical survival metrics from the Kaplan-Meier plotter platform (http://kmplot.com). The analysis was conducted using the default settings for the 'Breast Cancer' module, with the following key parameters: The 'autoselect best cut-off' option was applied to dichotomize patients into high and low G3BP1 expression groups, and the probe set '201503_at' was selected for G3BP1 quantification. Subtype-specific stratification was implemented for luminal A (ER+/PR+, HER2- and low Ki-67), luminal B (ER+/PR+, HER2- and high Ki-67 or HER2+), HER2-positive (ER-, PR- and HER2+) and basal-like (largely triple-negative: ER-, PR- and HER2-) using established classifier algorithms within the platform. Survival disparities across subgroups were statistically evaluated using the log-rank test, with $P<0.05$ being considered to indicate a statistically significant difference. To comprehensively evaluate the clinical impact of G3BP1 dysregulation in BRCA using multiple survival endpoints: Overall survival (OS), disease-free survival (DFS), distant metastasis-free survival (DMFS) and post-progression survival (PPS).

Differentially expressed genes (DEGs) analysis, volcano plot and heatmap. To identify the DEGs between the high G3BP1 and low G3BP1 expression groups, differential analysis was performed using the 'DESeq2' R package (https://bioconductor.org/packages/release/bioc/html/DESeq2.html) with a threshold set at $\log_2$ fold change (FC) >0.585 and false discovery rate (FDR) <0.05 (corresponding to a linear scale of >1.5-fold change). Similar methods have been used in previous bioinformatics research on breast cancers (15). DEGs were visualized through a volcano plot generated using the 'ggplot2' R package (https://cran.r-project.org/web/packages/ggplot2/). The x-axis of the volcano plot is labelled as 'log2 FoldChange' and the red and green dots represent the upregulated and downregulated genes that met the threshold, while the gray dots represent the genes that did not meet the threshold. Additionally, a heatmap was generated using the 'pheatmap' R package (https://cran.r-project.org/web/packages/pheatmap/) to further illustrate the expression patterns of these DEGs across all samples.

GSEA. Analysis was performed using the Kyoto Encyclopedia of Genes and Genomes (KEGG) pathway database, Gene Ontology (GO) gene sets, including cellular components (CC), biological processes (BP) and molecular functions (MF), hallmark gene sets and Immunologic Signature Database (ImmuneSigDB), obtained from the Molecular Signatures Database (MsigDB, version 7.5.1) through its official website (http://software.broadinstitute.org/gsea/downloads.jsp). The 'clusterProfiler' package (https://bioconductor.org/packages/release/bioc/html/clusterProfiler.html) in R software was used for GSEA. The analysis was performed with 1,000 permutations to ensure statistical robustness. Gene sets demonstrating a normalized enrichment score (NES) >1.0 and achieving a nominal P<0.05 (after FDR correction) were considered to be statistically significant. To validate GSEA-predicted pathway associations, co-expression patterns between G3BP1 and core PI3K/AKT/mTOR signaling molecules were analyzed using transcriptomic data from the TIMER2.0 resource (http://timer.cistrome.org/).

Immunological correlation analysis. To investigate the relationship between G3BP1 expression and TIME composition in BRCA, comprehensive immune cell infiltration analyses were performed. Firstly, Spearman's rank correlation was used to evaluate associations between G3BP1 mRNA levels and the infiltration abundance of 22 immune cell types derived using CIBERSORT deconvolution algorithms. Secondly, correlations between G3BP1 and six major immune cell subsets (B cells, $CD4^+$ T cells, $CD8^+$ T cells, neutrophils, macrophages and dendritic cells) were further validated using the TIMER database. To explore potential mechanisms of G3BP1-mediated immune evasion, its co-expression with the immune checkpoint molecule PD-L1, also known as cluster of differentiation 274 (CD274) was assessed via scatter plot analysis and Spearman's rank correlation in the TIMER database.

Clinical data collection and IHC staining. A total of 38 paired breast cancer specimens and matching adjacent non-neoplastic tissues were retrospectively collected from female patients (median age, 52 years; age range, 34-73 years) undergoing surgical resection at The Second Affiliated Hospital of Anhui Medical University (Hefei, China) between January 2013 and October 2014.

Inclusion criteria comprised: i) Histologically confirmed diagnosis of primary breast invasive carcinoma; ii) surgically resected tumor tissue and adjacent normal tissue pairs meeting predefined quality standards (tumor cellularity ≥30%; intact protein preservation); and iii) complete clinicopathological records.

Exclusion criteria comprised: i) Diagnosis of non-breast primary malignancies or synchronous dual primaries (except bilateral breast cancer); ii) incomplete clinical or outcome documentation; and iii) specimens not meeting the G3BP1 detection standards. The study protocol was approved by the Institutional Ethics Committee of The Second Affiliated Hospital of Anhui Medical University (approval no. YX2019-055) and written informed consent was obtained from all participants prior to tissue procurement.

The samples were fixed in 4% formaldehyde at room temperature for 24 h and subsequently embedded in paraffin. Serial sections of 4 μm thickness were prepared, followed by baking at 60˚C for 2 h, xylene dewaxing and gradient ethanol dehydration. Following dehydration, antigen retrieval was performed. Sections were then permeabilized with 0.1% Triton X-100 for 15 min and blocked with 5% bovine serum albumin (cat. no. A7906; Sigma-Adrich; Merck KGaA) at room temperature for 1 h to prevent non-specific binding. IHC staining was performed using a monoclonal antibody against G3BP1 (1:200; cat. no. GB115527; Wuhan Servicebio Technology Co., Ltd.) with incubation at 37˚C for 60 min, followed by application of the secondary antibody (1:200; cat. no. PV6000; Beijing Zhongshan Jinqiao Biotechnology Co., Ltd.) at 37˚C for 30 min. Diaminobenzidine was used for chromogenic development for 3 min, followed by hematoxylin counterstaining (performed at room temperature for 3 min) and gradient dehydration. The staining results were evaluated under an Olympus light BX53 microscope (Olympus Corporation; magnification, x200).

Two senior pathologists independently assessed the staining of breast cancer cells under high-power fields using a double-blind method. To enhance objectivity and reduce observer variability, digitized whole-slide images (WSIs) of stained sections were additionally analyzed using QuPath (https://qupath.github.io/) digital pathology software (version 0.6.0). G3BP1 exhibited cytoplasmic staining, with the staining intensity being scored as follows: 0, no staining; 1, faint yellow granules visible in cytoplasm; 2, brown-yellow granules visible in cytoplasm; and 3, dark brown granules visible in cytoplasm. A total of five representative high-power fields were selected, and the percentage of positive cells in each field was quantified: 0, negative; 1, <25%; 2, 26-50%; 3, 51-75%; and 4, >75%. The staining area score was divided by the staining intensity score. A score <4 points indicated low G3BP1 expression, while a score ≥4 points indicated high G3BP1 expression.

Using QuPath, automated cell detection and classification algorithms were applied to the WSIs to quantify the percentage of G3BP1-positive tumor cells and measure the average optical density (OD) of staining intensity across the entire tumor region or within annotated representative areas.

The QuPath-derived quantitative data (positive cell percentage and mean OD) were used to corroborate the semi-quantitative manual H-scores. Consistency between manual H-scores and QuPath quantification was assessed using Spearman's rank correlation and Bland-Altman analysis. The pre-defined thresholds for acceptable agreement were set as a Spearman's correlation coefficient (ρ) >0.8, indicating a very strong monotonic relationship, and a Bland-Altman bias <5%, indicating a negligible mean difference between the two methods. These thresholds are commonly adopted in digital pathology validation studies to ensure that automated quantification is both highly correlated with and metrically similar to expert manual assessment (16,17).

Furthermore, differential expression of G3BP1 between breast cancer tissue and matching adjacent non-tumor tissue was analyzed using IHC data curated from the HPA database (https://www.proteinatlas.org). Protein localization and staining intensity were assessed comparatively to validate tissue-specific G3BP1 dysregulation in BRCA.

Statistical analysis. Multi-omics data and clinical validation were integrated using a robust statistical framework. Differential expression of G3BP1 in BRCA compared with normal tissues was assessed through the aforementioned non-parametric tests (Mann-Whitney U and Wilcoxon paired tests) using TCGA and CPTAC data. Associations with clinicopathological features were evaluated using Kruskal-Wallis and Mann-Whitney U tests. For the analysis of associations between G3BP1 expression levels (high vs. low) and categorical clinicopathological variables, Fisher's exact test was employed. This test was chosen due to its appropriateness for small sample sizes and when the assumptions of the χ^2 test (such as expected count in >20% of cells being ≤5) are violated. Survival outcomes (OS, DFS, DMFS and PPS) were analyzed using Kaplan-Meier curves with log-rank tests and Cox regression to identify G3BP1 as an independent prognostic marker. DEGs were screened (log_2FC >0.585; FDR <0.05) and visualized using volcano plots ('ggplot2') and heatmaps ('pheatmap'). GSEA with 'clusterProfiler'-identified pathways was carried out using KEGG, GO and hallmark gene sets (1,000 permutations; FDR <0.05; NES >1.0). Immune infiltration correlations were analyzed using Spearman's rank (CIBERSORT/TIMER). For G3BP1 protein expression in BRCA compared with normal tissues, statistical analysis was performed using the Wilcoxon signed-rank test (paired non-parametric test). For recurrence and metastasis risk assessment, multivariate Cox proportional hazards models were constructed to adjust for clinically relevant covariates including age and comorbidities, with hazard ratios (HR) and 95% confidence intervals (CI) calculated to quantify prognostic effects. All analyses were performed in R software with a two-tailed P<0.05, ensuring methodological rigor and reproducibility.

Results

G3BP1 is upregulated in BRCA. Integrated multi-omics analyses revealed significant upregulation of G3BP1 in BRCA tissue compared with normal tissue. Transcriptomic data from the TIMER database demonstrated elevated G3BP1 mRNA levels across multiple cancer types, including BRCA (Fig. 1A). Analysis of TCGA datasets confirmed that G3BP1 mRNA expression was significantly higher in primary tumor tissues compared with normal breast tissue controls ($P=3.82x10^{-12}$ vs. normal; Fig. 1B). Subtype stratification of TCGA samples showed significant upregulation in the luminal subtype (luminal A and B combined; $P=4.33x10^{-15}$ vs. normal) and triple-negative breast cancer (P=0.012 vs. Normal; Fig. S1A) subtypes, while HER2-positive tumors exhibited no significant difference (P=0.109 vs. normal; Fig. S1A). At the protein level, the CPTAC database showed increased G3BP1 abundance in BRCA tumors ($P=1.04x10^{-8}$ vs. normal; Fig. 1C), with significant elevation observed across all molecular subtypes (luminal, $P=1.30x10^{-8;}$ HER2-positive, P=0.019; TNBC, P=0.010 vs. normal; Fig. S1B). These proteomic findings were consistent with IHC validation from HPA, which revealed moderate cytoplasmic G3BP1 expression in tumor tissue ('medium staining'), whereas normal breast tissue exhibited minimal ('low') staining (Fig. 1D). Collectively, these results demonstrate G3BP1 is consistently upregulated in BRCA at both transcriptional and translational levels, highlighting its potential role in tumorigenesis.

Differential expression of G3BP1 across clinicopathological characteristics of BRCA. To elucidate the clinical relevance of G3BP1 in BRCA, G3BP1 expression was analyzed across key clinicopathological parameters using transcriptomic data from TCGA. G3BP1 mRNA levels exhibited stage-specific heterogeneity as T4 stage tumors demonstrated significantly elevated G3BP1 expression compared with T3 stage tumors (P=0.014), although no differences were observed between T4 and T1 (P=0.180) or T2 (P=0.071) stages (Fig. 2A). Notably, N2 stage tumors (characterized by extensive regional lymph node metastasis) showed markedly higher G3BP1 expression compared with N0 and N1 stages (P=0.005; Fig. 2B). This underscored its association with lymphatic progression. By contrast, G3BP1 expression was independent of pathological stage (I&II vs. III&IV; P=0.580; Fig. 2C) and distant metastasis (M0 vs. M1; P=0.200; Fig. 2D). Demographically, no significant associations were detected between G3BP1 expression and patient age (≤65 vs. >65 years; P=0.370; Fig. 2E) or sex (male vs. female; P=0.470; Fig. 2F). These findings suggest that G3BP1 overexpression is selectively associated with local tumor aggressiveness (stage T4) and advanced lymph node involvement (stage N2). The significant association with advanced T stage (local invasion) and N stage (lymphatic spread), coupled with the lack of association with distant metastasis (M stage) or overall pathological stage (which incorporates metastatic status), collectively implicated its role primarily in regional invasion rather than systemic dissemination.

High expression of G3BP1 is associated with poor prognosis in patients with BRCA. Survival analyses integrating multi-platform data demonstrated a notable association between elevated G3BP1 expression and unfavorable clinical outcomes in BRCA. Kaplan-Meier curves derived from TCGA cohorts revealed significantly shorter OS in patients with high G3BP1 expression compared with the low-expression group (P=0.037; Fig. 3A). External validation using the Kaplan-Meier plotter platform further corroborated these findings, showing

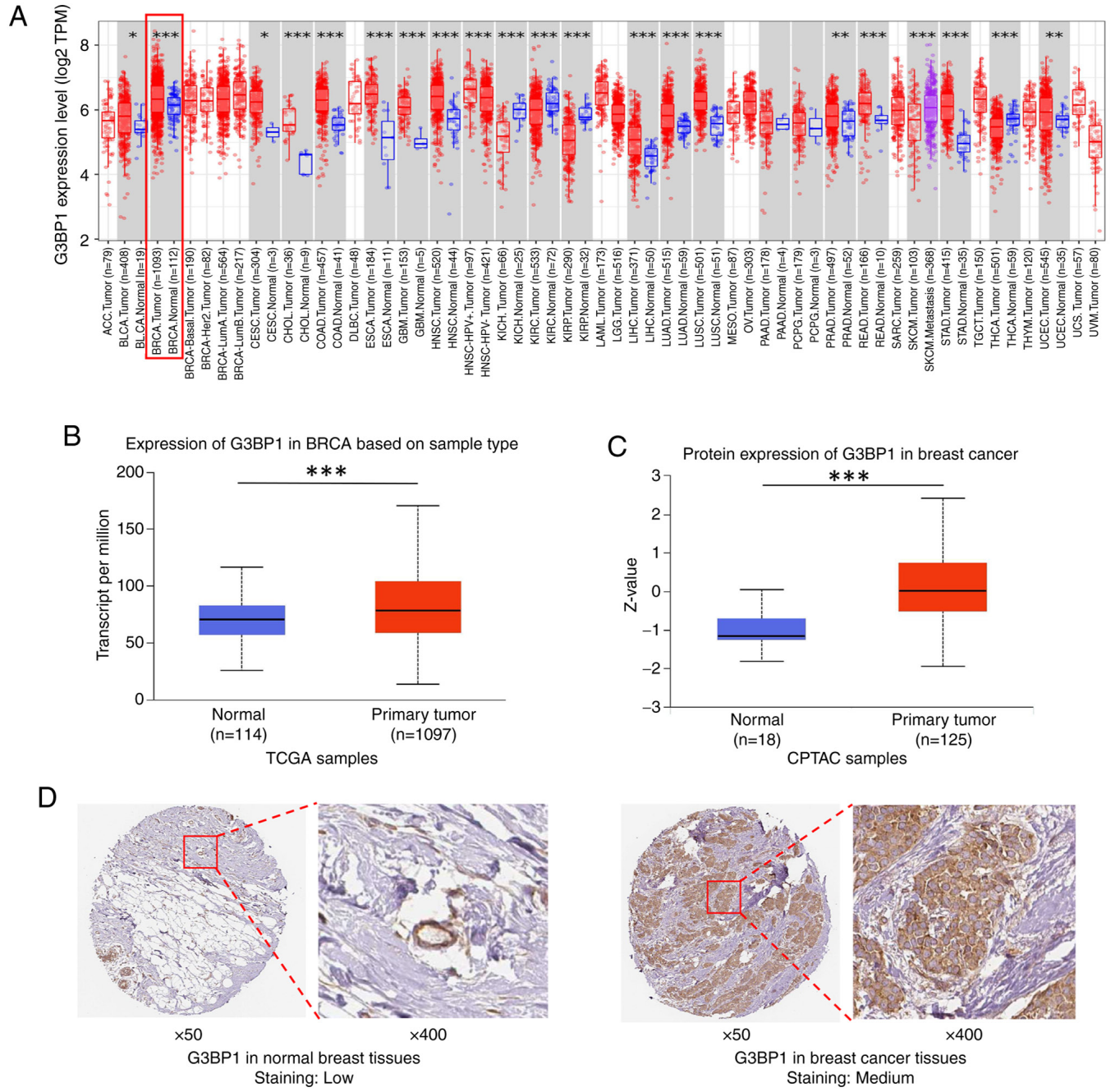

Figure 1. G3BP1 expression profile for both transcriptional and protein hierarchies in human tissues. (A) The G3BP1 mRNA expression in pan-cancers from the TIMER database. (B) Comparison of G3BP1 expression in normal and breast tumor tissues in TCGA database. (C) Comparison of G3BP1 expression in normal and breast tumor tissues in the CPTAC database, Z-value shows standard deviations from the median of BRCA samples. (D) Immunohistochemistry of G3BP1 in normal and cancerous breast tissues in the Human Protein Atlas dataset. *P<0.05; **P<0.01; ***P<0.001. TIMER, Tumor Immune Estimation Resource; CPTAC, Clinical Proteomic Tumor Analysis Consortium; BRCA, breast invasive carcinoma; TCGA, The Cancer Genome Atlas; G3BP1, Ras-GTPase-activating protein SH3 domain-binding protein 1; TPM, transcript per million.

that high G3BP1 levels were associated with reduced DFS (P=9.20x10^{-5}), DMFS (P=5.70x10^{-4}) and PPS (P=0.036; Fig. 3B-D).

In the Kaplan-Meier Plotter platform, survival analysis stratified by G3BP1 expression levels revealed distinct prognostic patterns across breast cancer subtypes (Fig. S2A-D). In the Luminal A cohort (Fig. S2A), high G3BP1 expression was significantly associated with worse OS (HR=1.36; 95% CI, 1.15-1.61; P=4.20x10^{-4}). A similar adverse prognostic trend was observed in luminal B tumors (Fig. S2B), where those with high G3BP1 expression exhibited reduced survival (HR=1.26; 95% CI, 1.04-1.53; P=0.010). By contrast, HER2-positive tumors (Fig. S2C) showed no statistically significant difference in survival between expression groups (HR=1.37; 95% CI, 0.94-2.00; P=0.110). In patients with basal/TNBC (Fig. S2D), high *G3BP1* expression was significantly associated with a worse DFS (HR=1.59; 95% CI, 1.25-2.01; P=1.10x10^{-4}).

G3BP1-associated molecular signatures and pathway enrichment in BRCA. To uncover the molecular mechanisms

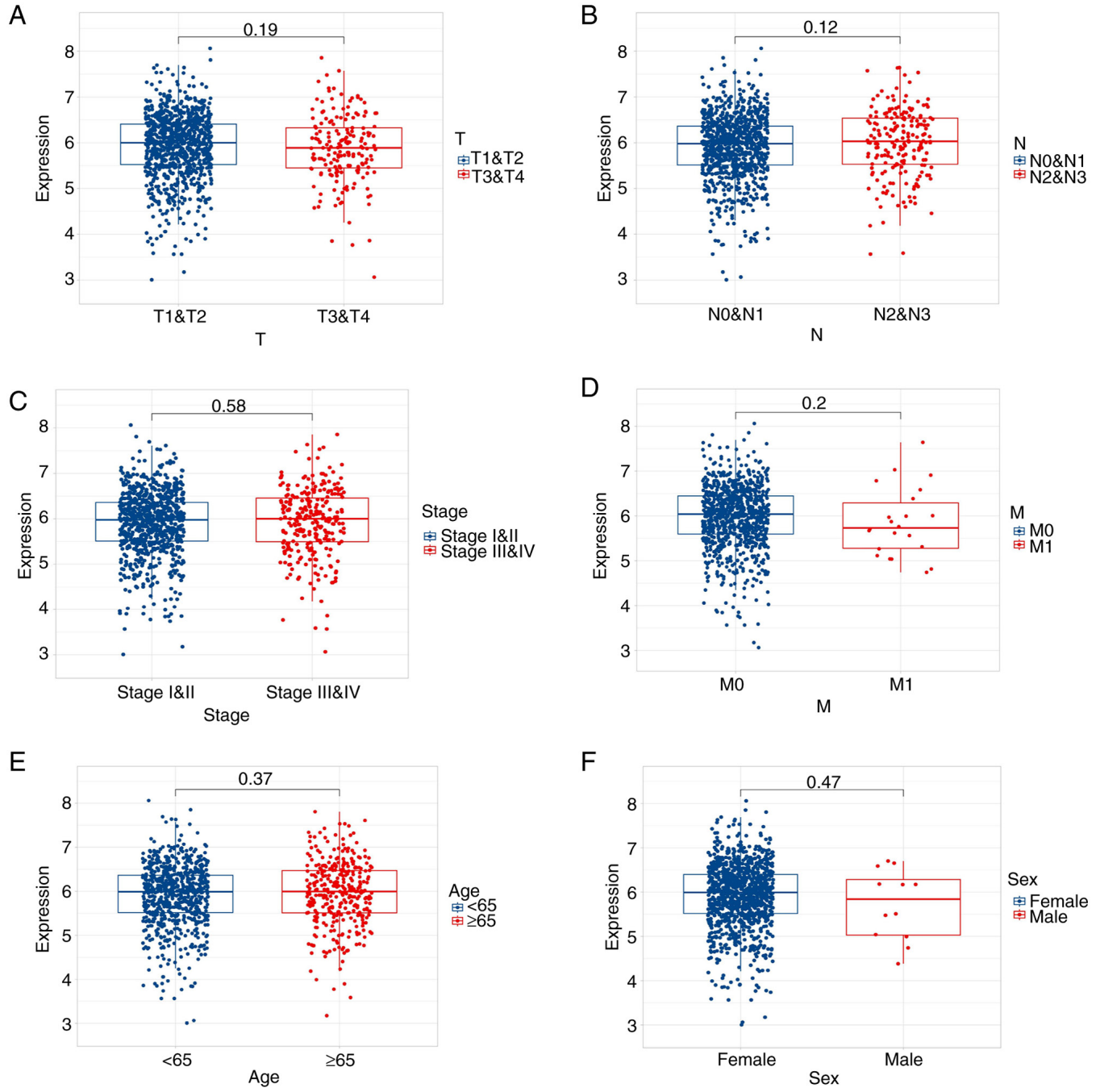

Figure 2. Association between G3BP1 expression levels and clinicopathological characteristics in BRCA. (A) T stage, (B) N stage, (C) pathological stage, (D) M stage, (E) age and (F) sex. T, tumor; N, lymph node; M, metastasis; G3BP1, Ras-GTPase-activating protein SH3 domain-binding protein 1.

underlying G3BP1-driven progression of BRCA, DEGs between G3BP1-high and G3BP1-low expression groups were systematically identified using TCGA datasets. Under strict thresholds (log_2FC >0.585; FDR <0.05), 67 genes were identified as markedly upregulated, while nine genes were downregulated. A volcano plot was used to visualize the distribution of DEGs, with red and green dots representing upregulated and downregulated genes, respectively (Fig. 4A). A heatmap further outlined the expression patterns of DEGs across samples, revealing coordinated activation of pro-tumorigenic genes [such as leptin (LEP), vascular endothelial growth factor D (VEGFD) and fatty acid binding protein 4 (FABP4)] in the high G3BP1 expression group (Fig. 4B).

The results of the GSEA are presented, focusing only on pathways with a NES >1 and an FDR of <0.05. The findings indicate significant enrichment in pathways such as PI3K/AKT/mTOR (NES=2.0605; P=0.0020) and ubiquitin-mediated protein hydrolysis (NES=2.7085; P<0.0001), as shown in Fig. 4C. Additional key enriched pathways in the high G3BP1 expression group are also presented in Fig. 4C. Furthermore, the top five pathways with NES >1 along with their statistical metrics have been listed in Table SI. These findings suggest that G3BP1 promotes BRCA progression by activating oncogenic pathways (such as PI3K/AKT/mTOR), disrupting proteostasis and modulating nuclear complex dynamics. The convergence of DEGs and enriched pathways

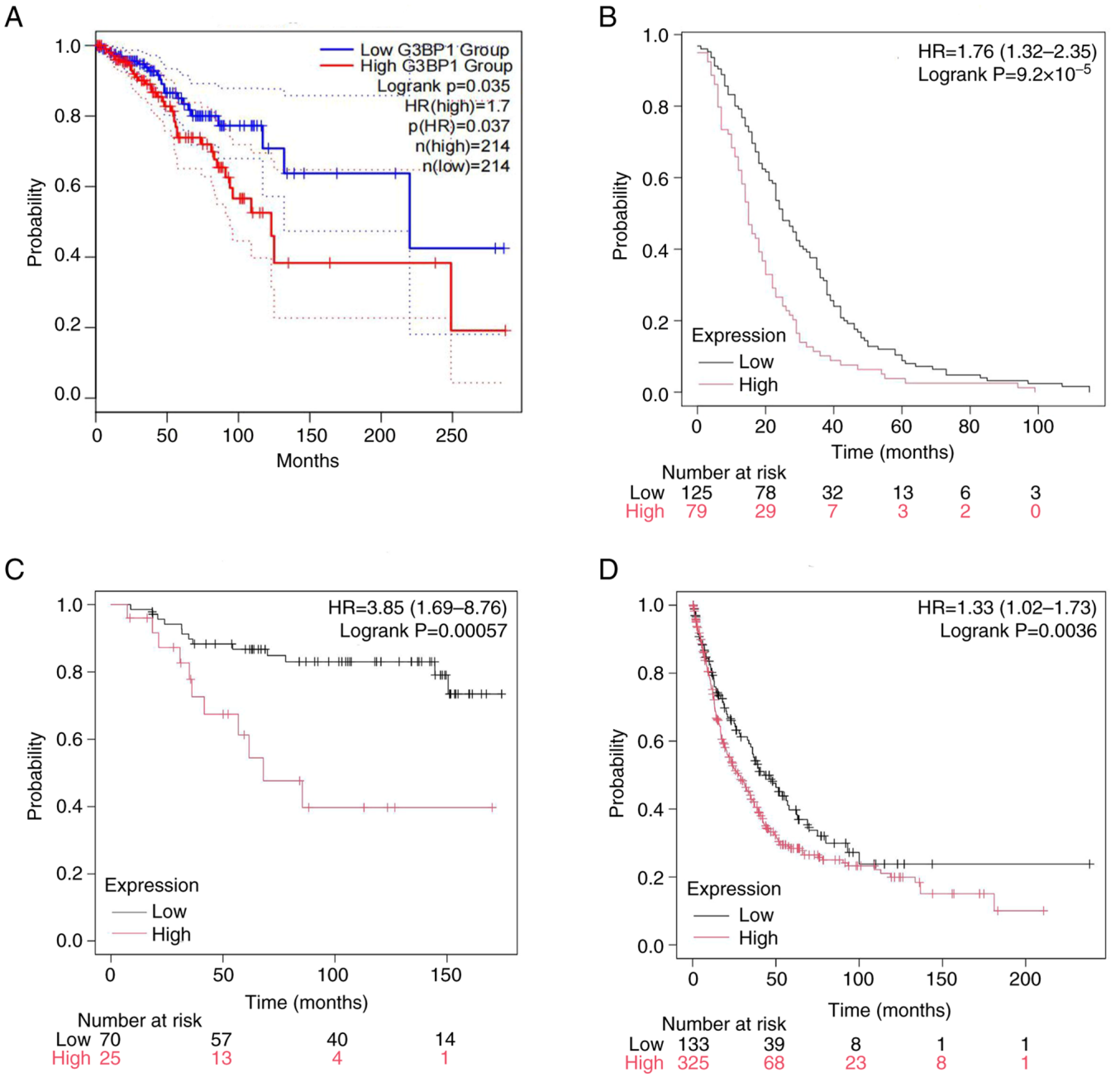

Figure 3. High G3BP1 expression is closely related to a poor prognosis in BRCA. (A) The survival analysis results from TCGA database showed that overall survival of the high expression group was markedly worse compared with the low expression group. (B) The survival analysis results from Kaplan-Meier plotter database showed that DFS of the high expression group was also markedly worse compared with the low expression group. (C) The survival analysis results from Kaplan-Meier plotter database showed that DMFS of the high expression group was also markedly worse compared with the low expression group. (D) The survival analysis results from Kaplan-Meier plotter database showed that PPS of the high expression group was also markedly worse compared with the low expression group. G3BP1, Ras-GTPase-activating protein SH3 domain-binding protein 1; BRCA, breast invasive carcinoma; TCGA, The Cancer Genome Atlas; DFS, disease free survival; DMFS, distant metastasis-free survival; PPS, post-progression survival.

underscores the therapeutic potential of targeting G3BP1 in BRCA.

GSEA suggested a significant association between G3BP1 and the PI3K/AKT/mTOR pathway (FDR <0.05). To validate this finding, further analysis of the co-expression patterns of G3BP1 and core signaling molecules in the TIMER2.0 database was conducted (Fig. S3). G3BP1 exhibited a strong positive correlation with PIK3CA (encoding the PI3K α catalytic subunit; ρ=0.583; $P=3.98x10^{-101}$) and a moderate correlation with PIK3CB (encoding PI3K β; ρ=0.488; $P=6.31x10^{-67}$), indicating its differential regulation of PI3K subtypes. There was no significant correlation between AKT1 expression and G3BP1 (ρ=-0.014; P=0.638), but a significant positive association was observed between AKT2 (ρ=0.264, $P=4.69x10^{-19}$) and AKT3 (ρ=0.230; $P=1.13x10^{-14}$), revealing the selective regulation of G3BP1 on AKT subtypes. It was also observed that G3BP1 significantly correlated with the expression of mTOR (ρ=0.475; $P=6.9x10^{-63}$) and regulatory associated proteins of mTOR complex 1 (ρ=0.536; $P=7.83x10^{-83}$). Overall, G3BP1 may drive the activation of

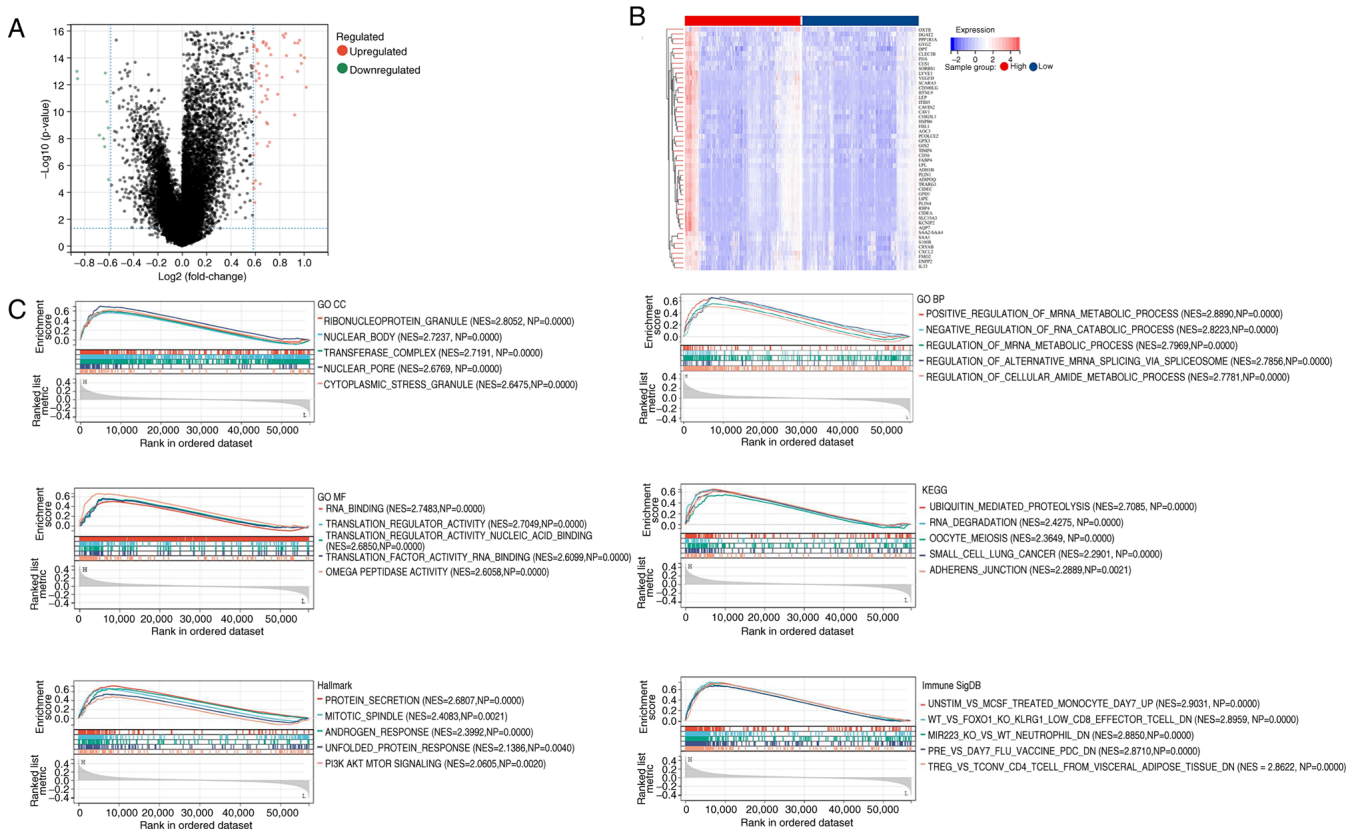

Figure 4. Multi-dimensional profiling of G3BP1-associated transcriptional dysregulation in breast invasive carcinoma. (A) Differential gene screening via volcano plot. (B) Stratified gene expression patterns by heatmap. (C) Multi-pathway gene set enrichment analysis including GO CC, GO BP, GO MF, KEGG, Hallmark and ImmuneSigDB. GO, Gene Ontology; CC, cellular components; BP, biological processes; MF, molecular functions; KEGG, Kyoto Encyclopedia of Genes and Genomes, G3BP1; Ras-GTPase-activating protein SH3 domain-binding protein 1; NES, normalized enrichment score; NP, nominal P-value.

PI3K/mTOR signaling by preferentially coordinating the PIK3CA-AKT2/AKT3 axis.

Relationship between G3BP1 expression, immune microenvironment and PD-L1 expression in BRCA. Survival of patients with breast cancer is associated with immune cell infiltration (16). The present study used Spearman's rank correlation analysis to examine the relationship between G3BP1 expression levels in BRCA and the infiltration of 22 immune cell types from CIBERSORT (Fig. 5A). The results showed that G3BP1 expression was positively correlated with 'neutrophils', 'T cells CD4 memory resting', 'macrophage M2', 'dendritic cells resting', 'T cells CD4 memory activated', 'masT cells resting', 'B cells naïve' and 'macrophages M1' (P<0.05), while it was negatively correlated with 'T cells regulatory', 'plasma cells', 'T cells CD8', 'B cells memory', 'natural killer (NK) cells activated' and 'T cells follicular helper' (P<0.001). Additionally, the present study evaluated the correlation between G3BP1 expression levels and the infiltration of six immune cell types in TIMER (Fig. 5B-E). The results demonstrated that G3BP1 expression was positively correlated with the infiltration of B cells, T cell $CD4^+$, T cell $CD8^+$, neutrophil, macrophage and dendritic cells (all P<0.05).

To identify the mechanistic link between G3BP1 and immune evasion, its relationship with PD-L1, also known as CD274, a critical immune checkpoint molecule, was evaluated. Based on the TIMER2.0 database, scatter plot analysis (Fig. S4) revealed a statistically significant positive correlation between G3BP1 and CD274 mRNA expression levels across BRCA samples (ρ=0.352; P=2.44x10^{-33}). The regression line with 95% CI demonstrated a progressive increase in G3BP1 expression with elevated CD274 levels. Data point density indicated clustering in the mid-range expression zone, with outliers extending to higher expression values. This significant correlation (P<0.001) indicates G3BP1-driven PD-L1 expression as a key mechanism for immune evasion in BRCA.

G3BP1 expression is upregulated in BRCA and associated with clinicopathology and adverse prognosis. IHC validation using 38 paired BRCA and adjacent normal tissues confirmed notable upregulation of G3BP1 in tumor tissues compared with normal tissues (P<0.001; Fig. 6A and B). The manual IHC scores and QuPath quantification of each patient are shown in Table SII, with consistency analysis indicating excellent consistency. Positive cell percentage showed near-perfect correlation (ρ=0.892; P<0.001) with minimal bias [-2.1%; 95% limits of agreement (LoA): -8.3 to +4.1%], while average OD exhibited stronger correlation (ρ=0.924; P<0.001) and negligible bias (+0.03; 95% LoA: -0.11 to +0.17). Both metrics exceeded predefined validation thresholds (ρ>0.8; bias <5%), confirming QuPath's reliability for standardized G3BP1 quantification (Table SIII).

Receiver operating characteristic (ROC) curve analysis further demonstrated the diagnostic potential of G3BP1, yielding

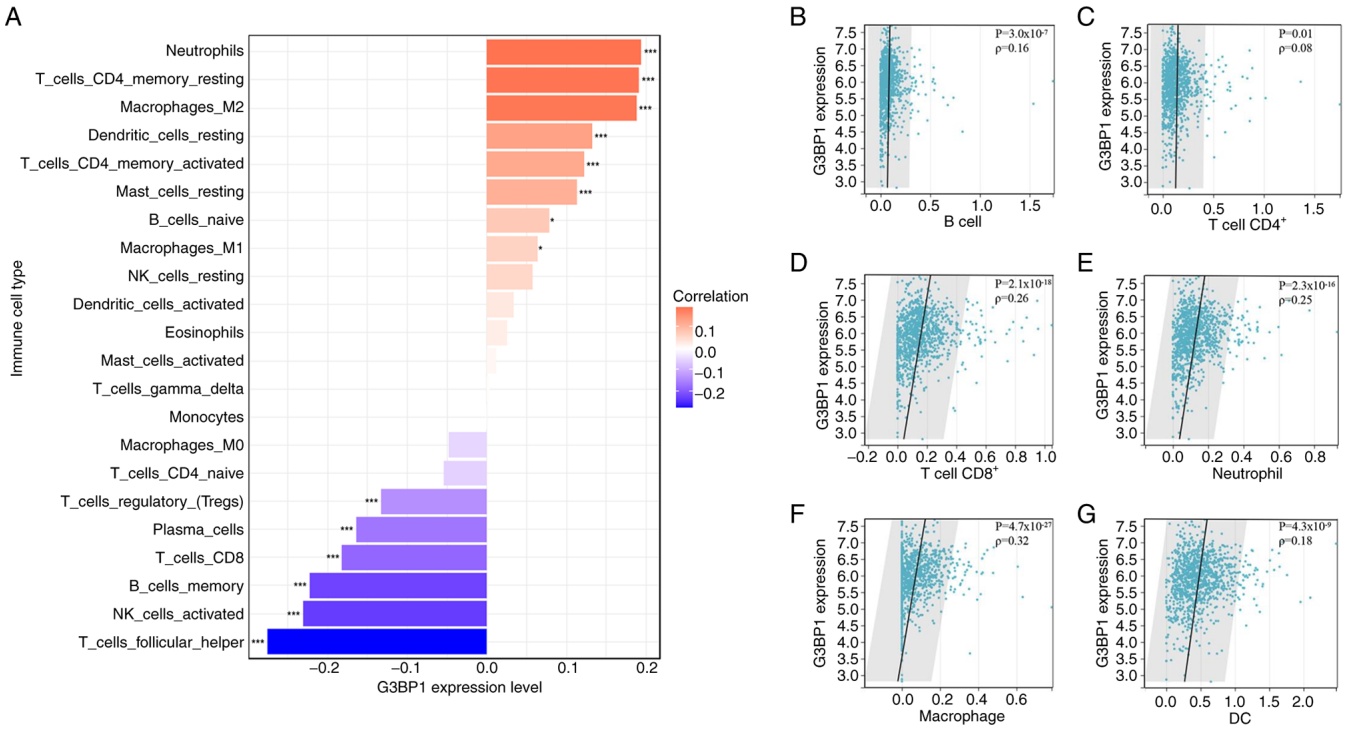

Figure 5. Correlation between immune cell infiltration and G3BP1 in BRCA. (A) Correlation between G3BP1 expression level in BRCA and infiltration of 22 immune cells. Relationship between G3BP1 expression and infiltration of (B) B cells, (C) T cells CD4+, (D) T cells CD8+, (E) neutrophils, (F) macrophages and (G) DCs in the TIMER database. *P<0.05 and ***P<0.001. BRCA, breast invasive carcinoma; DC, dendritic cells; G3BP1, Ras-GTPase-activating protein SH3 domain-binding protein 1.

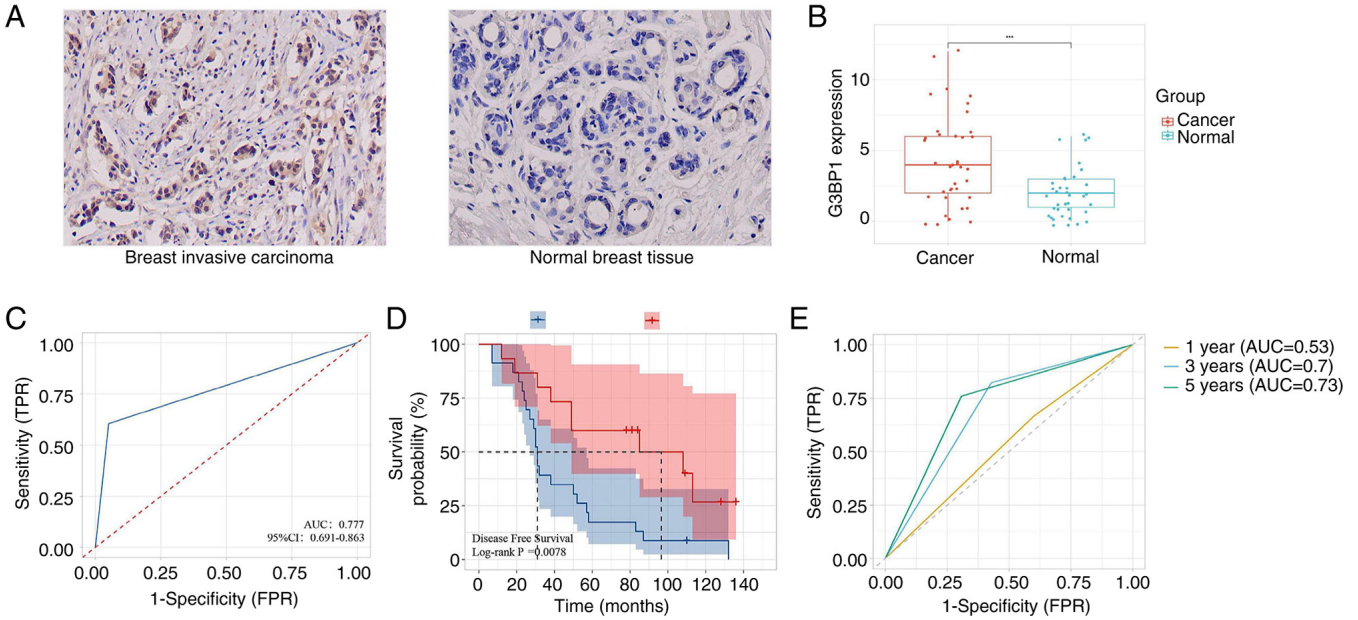

Figure 6. G3BP1 expression, prognosis and time-dependent ROC for BRCA. (A and B) G3BP1 protein was more expressed in BRCA compared with normal tissues, analyzed using immunohistochemistry. (C) The diagnostic value of G3BP1 expression in BRCA. (D) Kaplan-Meier survival analysis showed that upregulation G3BP1 had adverse DFS. (E) Time-dependent ROC curve of G3BP1 expression in predicting 1-, 3- and 5-year DFS. ***P<0.001. BRCA, breast invasive carcinoma; DFS, disease free survival; AUC, area under curve; G3BP1, Ras-GTPase-activating protein SH3 domain-binding protein 1; ROC, receiver operating characteristic; TPR, true positive rate; FPR, false positive rate.

an area under the curve (AUC) of 0.777 for distinguishing BRCA from normal tissues (Fig. 6C), indicating moderate diagnostic accuracy. Clinicopathological analysis revealed that elevated G3BP1 expression was significantly associated with advanced N stages (N2 and N3 vs. N0 and N1; P=0.003), higher pathological stages (stage III and IV vs. I and II; P=0.046), and tumor recurrence or metastasis (yes vs. no; P=0.010) (Table I). No significant associations were observed with age (P=0.285),

Table I. Association of G3BP1 expression and clinicopathologic characteristics.

Pathological characteristic	n	Low G3BP1 expression	High G3BP1 expression	P-value for Fisher's test
Age, years				0.285
<45	27	9	18	
≥45	11	6	5	
Menopausal status				0.280
Pre-menopause	34	12	22	
Menopause	4	3	1	
T stage				0.999
T1+T2	33	13	20	
T3+T4	5	2	3	
N stage				0.003
N0+N1	16	11	5	
N2+N3	22	4	18	
Pathological stage				0.046
I+II	17	10	7	
III	21	5	16	
Cardiovascular disease				0.999
No	34	12	22	
Yes	4	3	1	
Diabetes				0.509
No	35	15	20	
Yes	3	0	3	
Recurrence/metastasis				0.010
No	7	6	1	
Yes	31	9	22	

G3BP1, Ras-GTPase-activating protein SH3 domain-binding protein 1; T, tumor; N, lymph node.

menopausal status (P=0.280), T stage (P=0.999), cardiovascular disease (P=0.999) or diabetes (P=0.509), collectively indicating the specific role of G3BP1 in driving lymphatic metastasis, local progression and recurrence in breast cancer.

Kaplan-Meier survival analysis underscored the prognostic relevance of G3BP1, with high expression levels predicting significantly shorter DFS (P=0.007; Fig. 6D). Time-dependent ROC analysis further validated the prognostic usefulness of G3BP1, achieving AUC values of 0.530, 0.700 and 0.730 for predicting DFS at 1, 3 and 5-year intervals, respectively (Fig. 6E). After adjusting for age and complications (cardiovascular disease and diabetes), multivariate Cox regression analysis showed that the risk of recurrence or metastasis in the G3BP1 overexpression group significantly increased (HR=2.51; 95% CI, 1.07-5.90; P=0.034), supporting its independent value in the prognosis assessment of breast cancer (Table SIV). Collectively, the integration of multi-omics data and clinical validation solidifies G3BP1 as a critical molecular driver linked to tumor aggressiveness and unfavorable prognosis in BRCA.

Discussion

The present study comprehensively investigated the clinical significance and biological implications of G3BP1 in BRCA through integrated bioinformatics analysis and IHC validation. The present findings demonstrated that G3BP1 is markedly overexpressed in BRCA tissues at both mRNA and protein levels, and its high expression is associated with advanced T stage, lymph node metastasis and a poor prognosis. These results aligned with emerging evidence that G3BP1, as a critical RBP serves an oncogenic role in multiple cancers by regulating SG formation, mRNA metabolism and signaling pathways such as PI3K/AKT/mTOR and ubiquitin-mediated proteolysis (7,18).

Survival analyses from TCGA and Kaplan-Meier plotter databases consistently revealed that high G3BP1 expression predicted worse OS, DFS, DMFS and PPS in patients with BRCA. These findings were supported by IHC validation in the present clinical cohort, whereby elevated G3BP1 expression was markedly associated with aggressive clinicopathological features, including advanced N stage and pathological stage. ROC curve analysis further emphasized the diagnostic potential of G3BP1, with an AUC of 0.777, suggesting its usefulness in distinguishing BRCA from normal breast tissue, consistent with previous studies on its diagnostic role in other malignancies (19,20). Furthermore, time-dependent ROC analysis demonstrated that the predictive efficacy of G3BP1 for 5-year DFS (AUC=0.700) was

markedly superior to that of 1-year prognosis (AUC=0.530), indicating its greater suitability for medium-to-long-term prognostic evaluation.

GESA provided critical insights into the biological pathways modulated by G3BP1 in BRCA. The enrichment of ubiquitin-mediated proteolysis, PI3K/AKT/mTOR signaling and protein secretion suggested that G3BP1 may drive tumor progression by dysregulating protein homeostasis and oncogenic signaling networks (7,21). The PI3K/AKT/mTOR pathway in particular, is an established driver of breast cancer cell proliferation, therapy resistance and metastasis (22), further supporting the role of G3BP1 in promoting aggressive tumor behavior. Additionally, immune infiltration analysis revealed a complex relationship between G3BP1 expression and the TIME. G3BP1 exhibited a positive correlation with immunosuppressive cell types (for example, macrophage M2 and neutrophils) and a negative association with cytotoxic immune cells (for example, $CD8^+$ T and NK cells). This suggested that G3BP1 may contribute to an immune-evasive phenotype, potentially explaining its association with a poor prognosis. Recent studies implicated RBPs in modulating immune checkpoint molecules (such as PD-L1) and cytokine signaling (23,24), suggesting G3BP1 could influence immunotherapy responses, a hypothesis warranting further investigation.

The present data demonstrated that high G3BP1 expression was significantly associated with advanced N stage in BRCA, implicating its role in promoting lymphatic metastasis. A recent study reported that G3BP1 expression was notably upregulated in breast cancer and that knockdown of G3BP1 suppressed the proliferation and metastasis of breast cancer cells (25). In addition, G3BP1 has been shown to promote the progression of nasopharyngeal carcinoma (NPC) by activating the Janus kinase 2/STAT3 signaling pathway, which is associated with lymph node metastasis and a poor prognosis in patients with NPC (19). Additionally, in non-small cell lung cancer, G3BP1 was shown to interact with DEAH-Box Helicase 38 to activate the MAPK pathway and EMT, promoting tumor cell migration and invasion, thereby increasing the risk of lymph node metastasis (26). Subsequently, TIMER pan-cancer analysis revealed G3BP1 upregulation in 18 out of 33 cancer types, including cervical squamous cell carcinoma and endocervical adenocarcinoma, stomach adenocarcinoma and lung adenocarcinoma, which frequently exhibit lymphatic spread. Targeting G3BP1 may thus represent a pan-cancer therapeutic strategy against lymphatic metastasis.

To the best of our knowledge, the present study is among the first to systematically link G3BP1 to BRCA progression using multi-omics approaches. The consistency between TCGA data and the present IHC results strengthened the reliability of the conclusions drawn. Notably, the role of G3BP1 in SG formation may also explain its upregulation in BRCA. Cancer cells frequently encounter metabolic and oxidative stress, and G3BP1-mediated SG assembly could enhance tumor cell survival under such conditions (27,28). This adaptive mechanism may contribute to chemotherapy resistance, a hypothesis supported by the observation that high G3BP1 levels were associated with worse PPS. The translational potential of G3BP1 lies in its dual role as a diagnostic and therapeutic target. Due to its overexpression in tumor tissues, G3BP1 could be used for liquid biopsy-based detection of early-stage BRCA. Moreover, small-molecule inhibitors targeting the RNA-binding domains of G3BP1 or its interaction with SG components (for example, ubiquitin-specific peptidase 10 and caprin 1) may offer novel therapeutic avenues (29,30). Preclinical studies in other cancer types showed that G3BP1 knockdown suppresses tumor growth (17,19,24), supporting its candidacy for targeted therapy in BRCA.

To directly resolve whether the pathway associations of G3BP1 are primarily mediated through SGs or via direct molecular interactions, future studies should employ SG perturbation assays using CRISPR-mediated knockout of core SG components [such as T cell intracellular antigen 1 (TIA-1)] and pharmacological-integrated stress response inhibitors in BRCA cell lines, followed by a comprehensive assessment of PI3K/AKT pathway activity. With this, spatiotemporal mapping through live-cell Förster resonance energy transfer imaging should distinguish direct cytosolic binding from SG-dependent interactions between G3BP1 and PI3K regulators. Functional validation using SG-defective G3BP1 mutants in isogenic knockout models should establish causal relationships, while clinical correlation of SG markers (such as TIA-1 and eukaryotic initiation factor 3 subunit η) with PI3K activation signatures in BRCA samples using multiplex IHC should confirm translational relevance (31-33).

The present study showed several limitations that warrant discussion. Firstly, the IHC validation cohort (n=38) derived from a single-center retrospective cohort may have limited the statistical power for subgroup analyses. The present study acknowledges that expanding sample size through multi-center collaborations (for example, >100 paired samples) is essential to validate the association between G3BP1 expression and breast cancer. Secondly, the retrospective design carried inherent risks of selection bias. Future prospective studies incorporating longitudinal treatment response data could further strengthen the clinical utility of G3BP1 as a prognostic biomarker. Thirdly, the lack of clinically annotated cohorts receiving targeted therapies (for example, PI3K inhibitors) or immunotherapy limited the direct exploration of the predictive value of G3BP1. Fourthly, experimental validation using small-interfering RNA/CRISPR models and *in vivo* systems is essential to confirm the functional mechanisms of G3BP1 (for example, the PI3K/AKT/mTOR pathway). Investigating the interaction between G3BP1 and immune cells via co-culture experiments, including macrophage polarization and T cell inhibition assays, is equally important. Addressing these gaps could substantially strengthen the scientific foundation for translating G3BP1 into clinical applications, potentially facilitating its development as both a diagnostic biomarker and a therapeutic target in precision oncology.

In conclusion, the present study identified G3BP1 as a critical prognostic biomarker in BRCA, with elevated expression strongly associated with advanced tumor progression and diminished survival outcomes. However, the small IHC validation cohort (n=38) constrained subtype-specific generalization and bioinformatics-predicted mechanisms (for example, PI3K/AKT activation and immune evasion) require further functional validation. Future multicenter cohorts and

experimental models should address these gaps and evaluate the translational potential in precision oncology frameworks.

Acknowledgements

Not applicable.

Funding

The present study was supported by the Research Fund of Anhui Institute of Translational Medicine (grant no. 2023zhyx-C65), Anhui Provincial Health Scientific Research Project (grant nos. AHWJ2024BAb30020 and AHWJ2023BAb20009) and Postgraduate Innovation Research and Practice Program of Anhui Medical University (grant no. YJS20240102).

Availability of data and materials

The data generated in the present study may be requested from the corresponding author.

Authors' contributions

JJL conceptualized the present study and was involved in data curation (processing and annotating clinical and pathological data from the internal patient cohort), formal analysis, methodology, writing, reviewing and editing. ZQZ was also involved in conceptualization, data curation (collecting and organizing raw multi-omics data from public databases), formal analysis and writing the original draft. JS was involved in formal analysis, validation and writing the original draft. JHW was involved in data curation (standardizing and validating IHC image data and associated clinical metadata), methodology, validation and writing the original draft. XZ was involved in data analysis, interpretation and writing the original draft. WS was involved in the methodology and validation. JL was involved in methodology, and validation. HZ was involved in funding acquisition and methodology. YWY was involved in funding acquisition, methodology, supervision and visualization. FFL was involved in conceptualization, funding acquisition, methodology, supervision, visualization, writing and editing. JJL and FFL confirm the authenticity of all the raw data. All authors read and approved the final version of the manuscript.

Ethics approval and consent to participate

All procedures followed the ethical guidelines of the Declaration of Helsinki in 1964 and its subsequent amendments. The study received approval from the Ethics Committee of the Second Affiliated Hospital of Anhui Medical University (approval no. YX2019-055). This study declares that written informed consent was obtained from all participating patients.

Patient consent for publication

Not applicable.

Competing interests

The authors declare that they have no competing interests.

References

1. Newman L: Oncologic anthropology: Global variations in breast cancer risk, biology, and outcome. J Surg Oncol 128: 959-966, 2023.
2. Abdulla RA, Kareem NA, Assadi RA, Sanaullah AAR, Nandagopal S, Wazil SM and Muttappallymyalil J: Impact of breast cancer awareness program on breast screening utilization among women in the United Arab Emirates: A cross-sectional study. BMC Public Health 25: 578, 2025.
3. Carlson RW, Allred DC, Anderson BO, Burstein HJ, Carter WB, Edge SB, Erban JK, Farrar WB, Forero A, Giordano SH, *et al*: Invasive breast cancer. J Natl Compr Canc Netw 9: 136-222, 2011.
4. Ihle CL, Wright-Hobart SJ and Owens P: Therapeutics targeting the metastatic breast cancer bone microenvironment. Pharmacol Ther 239: 108280, 2022.
5. Baumann Z, Auf der Maur P and Bentires-Alj M: Feed-forward loops between metastatic cancer cells and their microenvironment-the stage of escalation. EMBO Mol Med 14: e14283, 2022.
6. Wang L, Sun M, Yang S, Chen Y and Li T: Intraoperative radiotherapy is not a better alternative to whole breast radiotherapy as a therapeutic option for early-stage breast cancer. Front Oncol 11: 737982, 2021.
7. Guo J, Huang R, Mei Y, Lu S, Gong J, Wang L, Ding L, Wu H, Pan D and Liu W: Application of stress granule core element G3BP1 in various diseases: A review. Int J Biol Macromol 282: 137254, 2024.
8. Sun M, Liu X, Xia L, Chen Y, Kuang L, Gu X and Li T: A nine-lncRNA signature predicts distant relapse-free survival of HER2-negative breast cancer patients receiving taxane and anthracycline-based neoadjuvant chemotherapy. Biochem Pharmacol 189: 114285, 2021.
9. Zhang L, Gu S, Wang L, Zhao L, Li T, Zhao X and Zhang L: M2 macrophages promote PD-L1 expression in triple-negative breast cancer via secreting CXCL1. Pathol Res Pract 260: 155458, 2024.
10. Zhang J, Ye CX, Chen HT, Li T, Ma LT and Guo Y: Jianpi-Tiaoqi decoction inhibits tumour proliferation and lung metastasis in tumour-bearing mice with triple-negative breast cancer. Clin Exp Pharmacol Physiol 51: e13900, 2024.
11. Hashemi M, Taheriazam A, Daneii P, Hassanpour A, Kakavand A, Rezaei S, Hejazi ES, Aboutalebi M, Gholamrezaie H, Saebfar H, *et al*: Targeting PI3K/Akt signaling in prostate cancer therapy. J Cell Commun Signal 17: 423-443, 2023.
12. Tong W, Qin N, Lu T, Liu L, Liu R, Chen J and Luo N: Integrating bulk and single-cell RNA sequencing reveals SH3D21 promotes hepatocellular carcinoma progression by activating the PI3K/AKT/mTOR pathway. PLoS One 20: e0302766, 2025.
13. Li T, Fu J, Zeng Z, Cohen D, Li J, Chen Q, Li B and Liu XS: TIMER2.0 for analysis of tumor-infiltrating immune cells. Nucleic Acids Res 48: W509-W514, 2020.
14. Uhlén M, Fagerberg L, Hallström BM, Lindskog C, Oksvold P, Mardinoglu A, Sivertsson Å, Kampf C, Sjöstedt E, Asplund A, *et al*: Proteomics. Tissue-based map of the human proteome. Science 347: 1260419, 2015.
15. Zheng C, Guo H, Mo Y and Liu G: Integrating bioinformatics and drug sensitivity analyses to identify molecular characteristics associated with targeting necroptosis in breast cancer and their clinical prognostic significance. Recent Pat Anticancer Drug Discov 19: 681-694, 2024.
16. Aeffner F, Adissu HA, Boyle MC, Cardiff RD, Hagendorn E, Hoenerhoff MJ, Klopfleisch R, Newbigging S, Schaudien D, Turner O and Wilson K: Digital microscopy, image analysis, and virtual slide repository. ILAR J 59: 66-79, 2018.
17. Bankhead P, Loughrey MB, Fernández JA, Dombrowski Y, McArt DG, Dunne PD, McQuaid S, Gray RT, Murray LJ, Coleman HG, *et al*: QuPath: Open source software for digital pathology image analysis. Sci Rep 7: 16878, 2017.
18. Ali HR, Chlon L, Pharoah PD, Markowetz F and Caldas C: Patterns of immune infiltration in breast cancer and their clinical implications: A gene-expression-based retrospective study. PLoS Med 13: e1002194, 2016.
19. Ge Y, Jin J, Chen G, Li J, Ye M and Jin X: Endometrial cancer (EC) derived G3BP1 overexpression and mutant promote EC tumorigenesis and metastasis via SPOP/ERα axis. Cell Commun Signal 21: 303, 2023.
19. Zhan Y, Wang W, Wang H, Xu Y, Zhang Y, Ning Y, Zheng H, Luo J, Yang Y, Zang H, *et al*: G3BP1 interact with JAK2 mRNA to promote the malignant progression of nasopharyngeal carcinoma via activating JAK2/STAT3 signaling pathway. Int J Biol Sci 20: 94-112, 2024.

20. Xing FL, Li BR, Fang YJ, Liang C, Liu J, Wang W, Xu J, Yu XJ, Qin Y and Zhang B: G3BP2 promotes tumor progression and gemcitabine resistance in PDAC via regulating PDIA3-DKC1-hENT in a stress granules-dependent manner. Acta Pharmacol Sin 46: 474-488, 2025.
21. Guo J, Zhao Y, Sui H, Liu L, Liu F, Yang L, Gao F, Wang J, Zhu Y, Li L, *et al*: USP21-mediated G3BP1 stabilization accelerates proliferation and metastasis of esophageal squamous cell carcinoma via activating Wnt/β-Catenin signaling. Oncogenesis 13: 23, 2024.
22. Zhu K, Wu Y, He P, Fan Y, Zhong X, Zheng H and Luo T: PI3K/AKT/mTOR-targeted therapy for breast cancer. Cells 11: 2508, 2022.
23. Zhang Q, Yang Z, Hao X, Dandreo LJ, He L, Zhang Y, Wang F, Wu X and Xu L: Niclosamide improves cancer immunotherapy by modulating RNA-binding protein HuR-mediated PD-L1 signaling. Cell Biosci 13: 192, 2023.
24. Cook ME, Bradstreet TR, Webber AM, Kim J, Santeford A, Harris KM, Murphy MK, Tran J, Abdalla NM, Schwarzkopf EA, *et al*: The ZFP36 family of RNA binding proteins regulates homeostatic and autoreactive T cell responses. Sci Immunol 7: eabo0981, 2022.
25. Liu S, Tian S, Lin T, He X, Eze Ideozu J, Wang R, Wang Y, Yue D and Geng H: G3BP1 regulates breast cancer cell proliferation and metastasis by modulating PKCζ. Front Genet 13: 1034889, 2022.
26. Mi K, Zeng L, Chen Y, Ning J, Zhang S, Zhao P and Yang S: DHX38 enhances proliferation, metastasis, and EMT progression in NSCLC through the G3BP1-mediated MAPK pathway. Cell Signal 113: 110962, 2024.
27. Yao Z, Liu Y, Chen Q, Chen X, Zhu Z, Song S, Ma X and Yang P: The divergent effects of G3BP orthologs on human stress granule assembly imply a centric role for the core protein interaction network. Cell Rep 43: 114617, 2024.
28. Redding A and Grabocka E: Stress granules and hormetic adaptation of cancer. Trends Cancer 9: 995-1005, 2023.
29. Schulte T, Panas MD, Han X, Williams L, Kedersha N, Fleck JS, Tan TJC, Dopico XC, Olsson A, Morro AM, *et al*: Caprin-1 binding to the critical stress granule protein G3BP1 is influenced by pH. Open Biol 13: 220369, 2023.
30. Sheehan CT, Hampton TH and Madden DR: Tryptophan mutations in G3BP1 tune the stability of a cellular signaling hub by weakening transient interactions with Caprin1 and USP10. J Biol Chem 298: 102552, 2022.
31. Li Y, Xu C, Qian X, Wang G, Han C, Hua H, Dong M, Chen J, Yu H, Zhang R, *et al*: Myeloid PTEN loss affects the therapeutic response by promoting stress granule assembly and impairing phagocytosis by macrophages in breast cancer. Cell Death Discov 10: 344, 2024.
32. Yeong J, Tan T, Chow ZL, Cheng Q, Lee B, Seet A, Lim JX, Lim JCT, Ong CCH, Thike AA, *et al*: Multiplex immunohistochemistry/immunofluorescence (mIHC/IF) for PD-L1 testing in triple-negative breast cancer: A translational assay compared with conventional IHC. J Clin Pathol 73: 557-562, 2020.
33. Chen CH, Chen IC, Hsu CL, Lu TP, Wang MY, Tsai LW, Huang CS, Lu YS and Lin CH: Characterization of the tumor immune microenvironment in pregnancy-associated breast cancer through multiplex immunohistochemistry and transcriptome analyses. Breast Cancer Res 27: 154, 2025.